

Battery Charging With Model Predictive DPC based Converter Using Dynamic DC-link Reference

Abinash Rath

Department of Electrical Engineering
National Institute of Technology, Rourkela
Email- abinash_rath@nitrrkl.ac.in

Gopalakrishna Srungavarapu

Department of Electrical Engineering
National Institute of Technology, Rourkela
Email- gopal@nitrrkl.ac.in

Abstract— The wide use of the delicate Lithium-ion battery in electric vehicles (EVs), UPS, etc. needs delicate charging systems operating at high power quality. The Direct Power Control (DPC), owing to its quicker transient response, serves as a good alternative for the control of PWM rectifiers in a battery charging system that is integrated into the grid. The classical way of designing the charging system includes separate stages of rectification and charging voltage control (using dc-dc converters). This paper proposes a mechanism that uses a dynamic dc-link voltage reference in the PWM rectifier to eliminate the dc-dc converter from the conventional system. This results in reduced size, weight, and cost for the whole system because of fewer hardware requirements. To select the switching vector for the PWM rectifier, here the model predictive control is used because not only does it avoid additional PWM generation block but it also has the ability to be versatile enough to accommodate different non-linear constraints in its algorithm. To validate the proposed method, the simulation model is designed using MATLAB/Simulink and the results are presented.

Keywords— EV Battery Charging, Direct power control, CC/CV charging, Model predictive DPC (MP-DPC), Dynamic dc-link reference,

I. INTRODUCTION

Electric vehicles (EVs) are now popular because of their efficient features and environmental friendliness. Not only EVs, but the batteries find their applications in UPS, household inverters, etc. Hence the fast charging of these batteries is of large interest in recent times. The grid to vehicle (G2V) mode of operation allows the batteries to store energy obtained from the grid. In the vehicle to grid (V2G) mode of operation, the stored energy can also be sent back into the grid. When the battery is connected to the grid through a bidirectional converter, both modes of operation are possible [1].

The EVs mostly use Li-ion (Lithium-ion) batteries because of their capacity to produce high power, low rate of self-discharging, and high energy density (nearly twice of Ni-Cd). On the other hand, it requires a sensitive charging phenomenon as the aging of these batteries becomes an issue when it is subjected to frequent current alterations or large ripples in the current. These characteristics of the Li-ion batteries demand a stable charging unit that takes care of the battery life [2].

The introduction of the DPC to control the power converters has offered advantages like a fast dynamic response and a simpler control structure [3]. Integration of features like constant switching frequency operation by space vector modulation, using dynamic tables as per demand [4], [5] further enhances the ability of DPC to handle PWM rectifiers. The finite control set MPC (FCS-MPC) has been one of the finest DPC techniques because of its accuracy in control [3], [6]. Its ability to accommodate other non-linear constraints makes it more flexible than the other control

techniques of the predictive group [5]. Several modifications in the cost function like the reduction in dc-link voltage ripple, switching loss, and interaction between the active and reactive power control [7], etc are presented as an additional attribute in the control operation. However, the MPC requires higher computational efficiency from the executing processor.

Conventionally the chargers are controlled by using VOC for switching vector section and PI regulators for charging control. Recently, direct power controlled PWM rectifiers are in use in the EV charging stations as they are capable of quicker response during a transient [8]. The literature describes a model predictive controlled converter which is used to feed a dc-dc power converter that is capable of delivering power in both directions finally interconnects the battery and grid [1]. Deployment of an interleaved buck converter followed by a PWM rectifier which is controlled using the predictive DPC presents a valuable alternative for battery charging at a high active power level [2]. In the literature, the existing battery charging methods involving the DPC are followed by a dc-dc converter that forms stage II of the power converter system. The battery is finally connected to the grid via this two-staged power converter. Although recently in [9] single-stage direct power controlled charging system has been proposed, yet the use of an additional PWM block makes the design a complex one. Its inability to add non-linear constraints in the control algorithm also makes it less flexible.

This paper aims at designing a DPC-based grid-connected fast EV battery charging system that draws nearly sinusoidal current from the grid with lesser hardware requirements. The proposed method doesn't necessitate the use of the dc-dc converter, which regulates the charging voltage in the conventional method. Instead of using a static desired set value, here a time-varying in nature with the dc-dc converter, here the time-varying reference for the control of dc-link voltage is employed in the outer control loop of the DPC algorithm. This dc-side voltage is controlled so as to maintain a constant charging current through the battery. Thus the dc-dc (Buck converter) converter is abandoned. Elimination of this converter makes the design simpler. In addition to that, the hardware requirement is broadly reduced, which ultimately reduces the cost of the system.

II. EXISTING BATTERY CHARGER USING DPC

The orthodox method of a battery charging system using DPC PWM rectifier is presented in terms of control blocks in fig. 1. Basically in this method, the charging system involves of two distinct stages of power conversion. The first stage of the two stages converts the three-phase ac power to dc power where dc voltage is fixed and controlled by the MP-DPC algorithm [1]. The grid supplies the three-leg converter module through the line inductance (L). The momentaneous active power (p), and reactive power (q) are estimated from the stationary axis components of grid voltage and grid current using the instantaneous power theory. An objective function

comprising of the deviations in the active and reactive power is minimized to find the most appropriate switching combination [1].

In the second stage, dynamic referencing is used for the control of the dc-dc converter which connects the battery to the grid. It is the stage II which controls the battery input current and manages the power flow to or from the battery. As the active power flows in both directions of the battery, the power converter used in stage II has to be a bidirectional converter. For this, the controller continuously senses the battery current and evaluates the error by subtracting it from the desired set value of it. Depending on the obtained error, a pulse width modulation block evaluates the duty ratio of the PWM signal which controls the stage II power converter.

To further improve the power handling capacity, the deployment of the interleaved buck converter has been projected in [2]. If there are ‘ m ’ number of legs in the buck converter, it requires ‘ m ’ number of carrier waves so that each leg can be controlled independently. The carrier waves are generated at a phase difference of ‘ $2\pi/m$ ’. By adopting this structure the frequency of the change in current increases by a factor of ‘ m ’ which ultimately contributes in reducing the ripple to achieve smoother control.

However, it needs ‘ m ’ number of extra switching devices and inductors. The generation of multiple carrier signals and their control make the overall process a complex one.

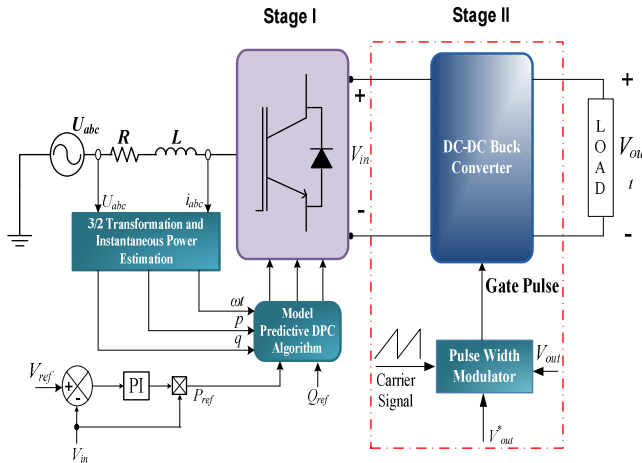


Fig. 1. Schematic of the orthodox DPC based battery charger

III. PROPOSED METHOD FOR BATTERY CHARGING

The proposed method presents a simple yet effective modification in the control structure which is able to eliminate the second stage (dc-dc converter) of the conventional charging system given in fig. 1. As the better performance of conventional DPC [10] is limited to only the set of circuit parameters upon which the switching table is designed, here an advanced and more accurate control method (MP-DPC) is chosen over the conventional DPC for better performance.

A. The Finite Control Set MPC (FCS-MPC)

The FCS-MPC is one of the simplest control structures in the model predictive control family. Here the system parameters like the active and reactive power gradients (p' and q') for all the switching vectors are predicted mathematically. These expressions can be obtained by following a simple derivation given in (1) - (3).

By applying the voltage balance equation on the grid side, the three-phase voltage (U), the supply current (i), and the converter end voltage vector (v) are related by (1).

$$U_{\alpha\beta} = i_{\alpha\beta}R + L \frac{di_{\alpha\beta}}{dt} + v_{\alpha\beta} \quad (1)$$

From the given expression in (1), the gradient of current can be expressed as (2).

$$\frac{di_{\alpha\beta}}{dt} = \frac{1}{L}(U_{\alpha\beta} - v_{\alpha\beta} - i_{\alpha\beta}R) \quad (2)$$

The complex power received from the grid can be expressed as (3). [11]

$$s = 1.5(i_{\alpha\beta}^* U_{\alpha\beta}) \quad (3)$$

Using (2) and (3), the expression for the gradient of the complex power can be obtained which is given in (4).

$$\frac{ds}{dt} = \frac{1}{L} \left[1.5 \left(|U_{\alpha\beta}|^2 - (v_{\alpha\beta}^* U_{\alpha\beta}) \right) - (R - j\omega L)s \right] \quad (4)$$

Separating the real and imaginary part of (4) the vector form expression for the active and reactive power gradients can be obtained which are given in (5).

$$p' = \frac{1}{L} \left[|U_{\alpha\beta}|^2 - \text{Re}(v_{\alpha\beta}^* U_{\alpha\beta}) \right] - \omega q - \frac{R}{L} p \quad (5)$$

$$q' = -\frac{1.5}{L} \text{Im}(v_{\alpha\beta}^* U_{\alpha\beta}) + \omega p - \frac{R}{L} q$$

This FCS-MPC requires the anticipated values of the control variables (p and q) at the following sample step. Using the instantaneous power theory, the active and reactive powers at the current sampling instant are estimated. From these values and their respective slopes, the future value can be predicted using Euler's approximation which is given in (6).

$$\left. \begin{aligned} p_{k+1} &= p + p' T_s \\ q_{k+1} &= q + q' T_s \end{aligned} \right\} \quad (6)$$

A cost function is framed as the distance between the points corresponding to the reference active and reference reactive powers (P^* , Q^*) and the predicted powers (p_{k+1} , q_{k+1}) for the next sampling instant on a p - q rectangular coordinate plane. This cost ‘ μ ’ is evaluated for all the switching vectors. The mathematical expression for the cost function is presented in (7).

$$\mu = \sqrt{(P^* - p_{k+1})^2 + (Q^* - q_{k+1})^2} \quad (7)$$

The switching voltage vector that refers to the least value of ‘ μ ’ is identified as the most appropriate choice among all available options of the switching voltage vectors.

To implement any of the converters in the real-time environment, a control delay is provided to allow the processor to collect samples of all the sensors and execute the vector selection algorithm which brings about inaccuracy in control. So here compensation is provided by using the two-step prediction of control variables rather than the single-step prediction as used in (6). So (p_{k+1} , q_{k+1}) are replaced by (p_{k+2} , q_{k+2}) in the cost function.

B. Generation of the time-varying dc-link reference

In this proposed method, rather than controlling the DC link voltage, the controller aims at controlling the current drawn from the dc side of the converter (the charging current) which is achieved by using an appropriate reference as the set point. The whole control structure is presented in fig. 2.

The change in the dc-link voltage is a reflection of the required change in the charging current. In order to achieve a fast charging rate and maintain good battery life, the rated battery current is chosen as the set point of the battery charging current (i_{ch}^*). The measured battery current (i_{ch}) is compared with i_{ch}^* and the generated error (Δi_{ch}) is fed to a PI controller. Mathematically ' Δi_{ch} ' can be expressed as (8).

$$\Delta i_{ch} = i_{ch}^* - i_{ch} \quad (8)$$

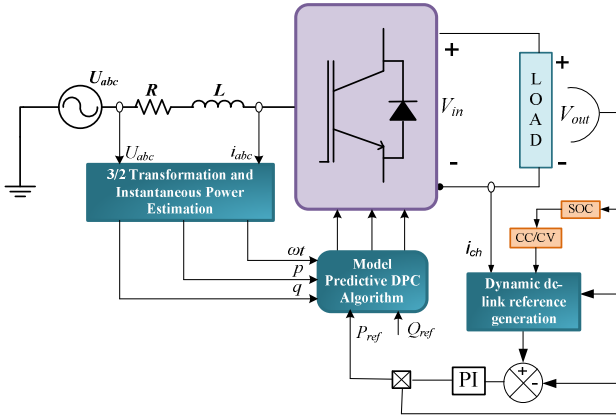


Fig. 2. Schematics of the proposed method

This PI controller regulates the battery charging current around its reference value. The output of the PI controller can be termed as the error in the reference dc-link voltage (ΔV_{ref}), which is added to the nominal desired value (V'_{ref}) of the voltage at the dc end to generate the time-varying setpoint of the dc voltage (V^*_{ref}). The mathematical expressions for ' ΔV_{ref} ' and ' V^*_{ref} ' are shown in (9) and (10), respectively.

$$\Delta V_{ref} = (k_p + \frac{k_i}{s}) \Delta i_{ch} \quad (9)$$

$$V^*_{ref} = V'_{ref} + \Delta V_{ref} \quad (10)$$

Replacing the expression of ' ΔV_{ref} ' in (10) which is obtained from (9), the ultimate mathematical equation for the time-varying dc-link reference can be obtained as shown in (11).

$$V^*_{ref} = V'_{ref} + (k_p + \frac{k_i}{s}) \Delta i_{ch} \quad (11)$$

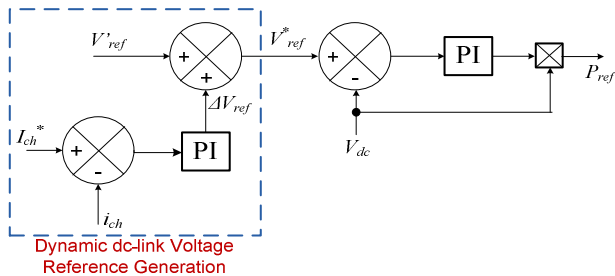


Fig. 3. Generation of the required time-varying dc-link reference

The whole process of this time-varying dc-link reference generation is depicted in a block diagram as shown in Fig. 3.

C. CC/CV Charging

This charging algorithm also employs the two well-known modes of charging, namely the constant current (CC) and constant voltage (CV) charging method of charging the Li-ion batteries. From the measured battery voltage, the state of charge (SOC) of the battery is estimated as per the mathematical model presented in [12].

When the SOC of the battery is more than 90%, it is considered that it is almost fully charged and the charging mode is switched from CC to CV. In the CC mode of charging, the objective remains to reduce the charging time by forcing a predetermined set value of charging current into the battery. The reference charging current is near about the nominal current rating of the battery. In CV mode the charging voltage is maintained at the maximum attainable voltage from the battery at 100% SOC. The charging current goes on decreasing with the rising SOC, and the charging process is terminated when the charging current reduces to its 10%. At this stage, the battery is considered to be fully charged and gets disconnected from the charging system. Adopting this CC/CV charging algorithm optimizes the charging time and battery life too [13].

IV. RESULTS

A computer simulation using MATLAB/Simulink is used to assess the utility of the suggested control strategy. In this simulation model, the Li-ion battery used has a nominal rating of 120 V and 6.33 A at the nominal voltage.

A few important parameters during the steady-state operation of the proposed battery charging system are displayed in Fig. 4. Fig. 4 (a) shows the waveforms of attenuated phase voltage by a factor of 2 and the phase current of the phase 'a'. A high displacement power factor can be seen as the zero crossings of both the waveforms coincide. Fig. 4 (b) shows the current waveforms of all three phases. Fig. 4 (c) presents the time-varying dc-link voltage of the active front end rectifier which is continuously changing in such a way that it is able to generate the desired charging current. Fig. 4 (d) shows the SOC of the battery which is seen to be rising as the battery is receiving active power. The fig. 4 (e) shows the waveforms of the p and q . The oscillation of ' q ' about 0 VAR again indicates the upf operation. The charging system draws active power at a mean of 844 W. The ripple content in the active power and reactive power are 28.48 W and 21.88 VAR, respectively. During the steady-state, these ripple contents are evaluated by calculating the standard deviations in the collected samples over 1 s. Fig. 4 (f) shows the battery current (i_{ch}) waveform. It can be observed to be oscillating around the i_{ch}^* of -6A. The negative value of i_{ch} indicates that the battery is consuming active power. To evaluate the power quality at the grid side, the spectra of the grid current are studied, which is estimated using FFT. The line current waveform in fig. 5 (a) depicts the waveshape of the current upon which FFT is performed. The obtained spectrum is shown in fig. 5 (b). The THD is found to be 3.94%.

Fig. 6 displays the waveforms of some physical parameters when the charging method is swapped from the CC to CV mode. As per the charging algorithm, when the battery attains 90% SOC, the charging mode is shifted to CV from CC. In CV mode a constant voltage slightly greater than

the battery voltage at 90% SOC is applied, so the charging rate drastically falls. This can be observed from the diminished slope in the SOC waveform. The active power now settles at a new steady-state which is much less than the steady state attained during CC mode. The reactive power continues its oscillation around '0' even in the CV mode. The charging

current immediately reduces to less than -1 A from -6. and the battery voltage reference is also reduced to 132 V as it is near to the maximum attainable voltage from the battery. The dc-link voltage can be observed to be accurately following the command to maintain 132V.

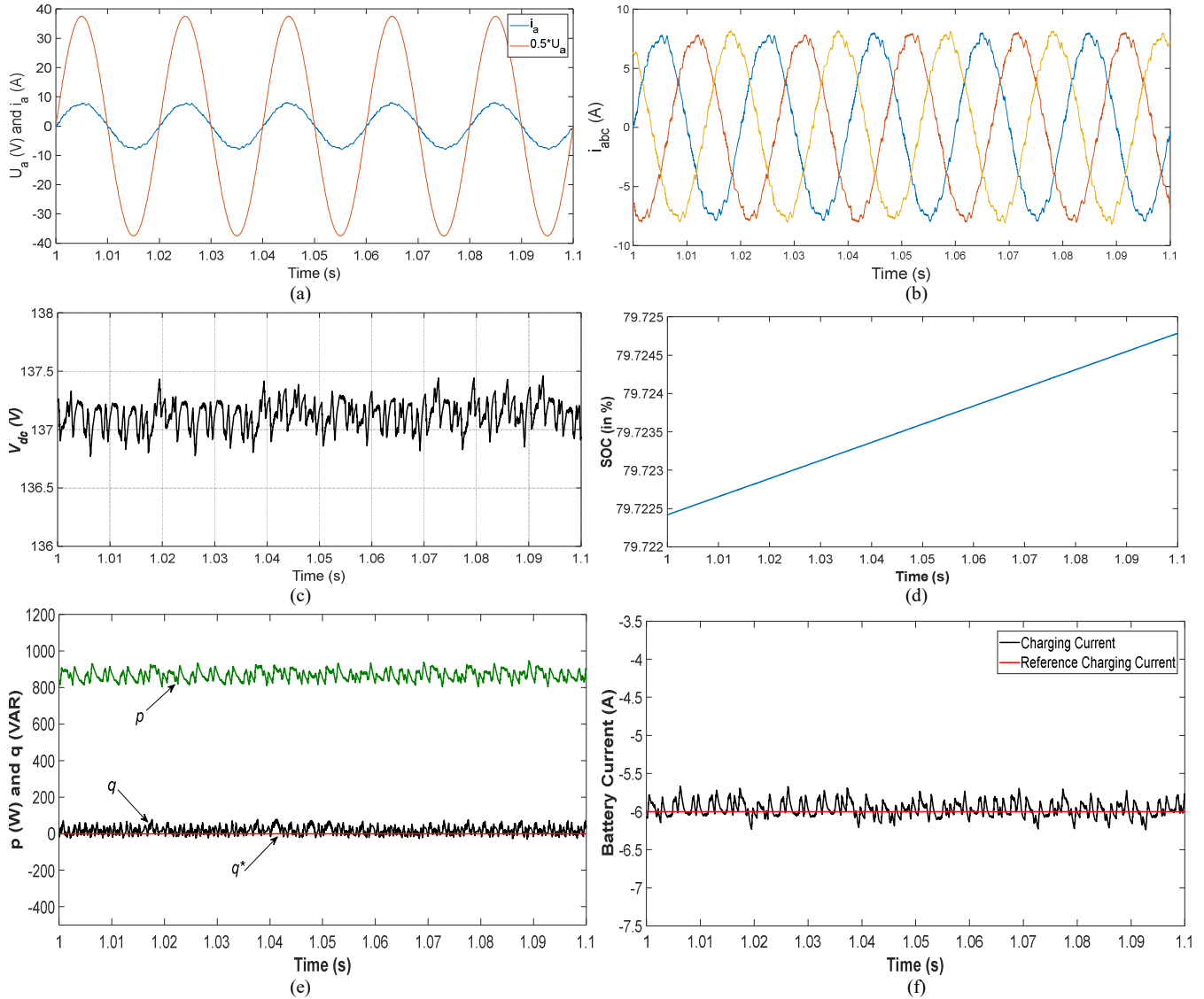


Fig. 4. Steady-state waveforms of the (a) phase voltage and current showing upf (b) Three-phase current, (c) dc-link voltage, (d) SOC, (e) instantaneous active and reactive power, (f) battery current

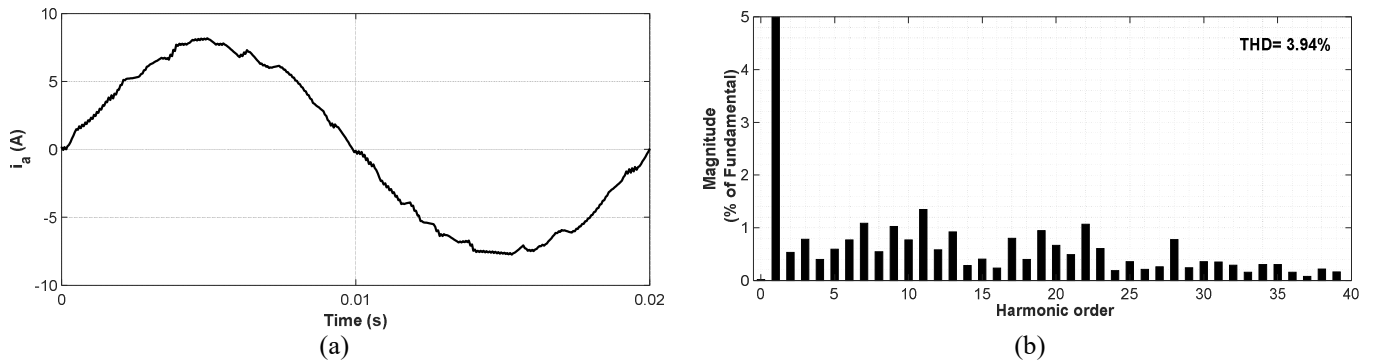


Fig. 5. The harmonic content analysis of the grid current (a) waveshape of i_a (b) spectrum of i_a

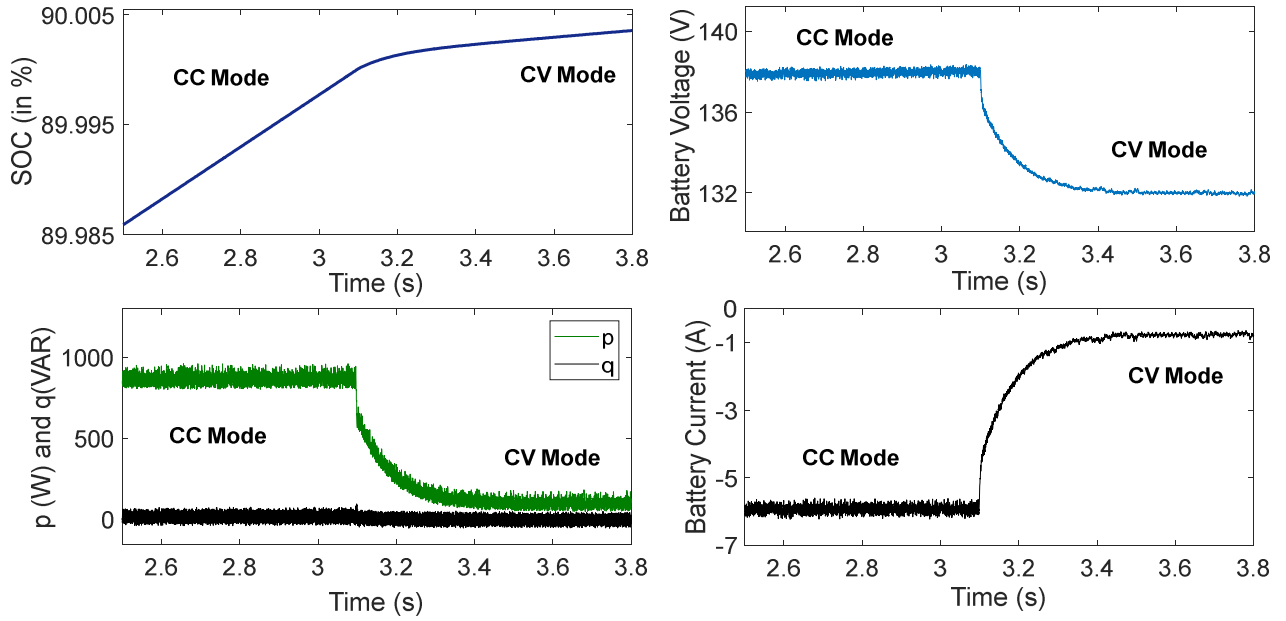


Fig. 6. Operation during the changeover from CC to CV mode (a) SOC, (b) Battery voltage, (c) active and reactive power (d) Battery current

For a comparative study, performance indices like the average THD in the source current (i_{abc}), ripple in the instantaneous active power (P_{rip}), and reactive power (Q_{rip}), and i_{ch} are tabulated in Table 1. Considering similar values of the performance indices obtained for the proposed method and the classical method, it can be ascertained that the technique using a time-varying reference of the dc-link voltage can be as effective as the existing method.

TABLE I. ANALYSIS AND PERFORMANCE EVALUATION

Performance Index	Classical Technique [2]	Proposed Technique
Average THD in i_{abc} (%)	3.79	3.94
P_{rip} (W)	28.07	28.48
Q_{rip} (Var)	22.64	21.78
i_{ch} (A)	0.088	0.090

V. CONCLUSION

This work has proposed a grid-connected fast EV battery charger that employs the FCS-MP-DPC technique and time-varying reference for the dc-link voltage control. From the parameters shown in the results section, it can be easily established that the proposed scheme has been successful at the abandonment of the dc-dc converter in the classical approach. The use of the DPC technique maintains fairly good power quality at the grid side, which is confirmed by the low THD value (3.94%) of the grid current. The proposed technique also maintains a low ripple in the waveforms of active power, reactive power, and also in the charging current highlighting the accuracy of the control technique. It not only raises the grid power quality but also helps the life of a Li-ion battery. As the proposed method achieves a reduction in the hardware requirement, the system size, weight, and more importantly the system cost are reduced.

APPENDIX

Symbols	Details	Numerical Values
U_{abc}	The three-phase voltages	70 V

R_s	Source resistance	0.2 Ω
L_f	Line inductance	12 mH
C	DC bus capacitance	2000 μ F
T_s	Sampling frequency	20 kHz

REFERENCES

- [1] T. He, M. Wu, D. D. C. Lu, R. P. Aguilera, J. Zhang, and J. Zhu, "Designed Dynamic Reference with Model Predictive Control for Bidirectional EV Chargers," *IEEE Access*, vol. 7, pp. 129362–129375, 2019, doi: 10.1109/ACCESS.2019.2940214.
- [2] H. W. Choi, S. M. Kim, J. Kim, Y. Cho, and K. B. Lee, "Deadbeat predictive direct power control of interleaved buck converter-based fast battery chargers for electric vehicles," *J. Power Electron.*, vol. 20, no. 5, pp. 1162–1171, 2020, doi: 10.1007/s43236-020-00106-7.
- [3] P. Cortés, J. Rodríguez, P. Antoniewicz, and M. Kazmierkowski, "Direct power control of an AFE using predictive control," *IEEE Trans. Power Electron.*, vol. 23, no. 5, pp. 2516–2523, 2008, doi: 10.1109/TPEL.2008.2002065.
- [4] A. Rath, A. Kumar, G. Srungavarapu, and M. Pattnaik, "Power quality improvement using 18 sector algorithm based direct power control," *Int. Trans. Electr. Energy Syst.*, no. April 2020, pp. 1–17, 2021, doi: 10.1002/2050-7038.12784.
- [5] A. Rath, G. Srungavarapu, and M. Pattnaik, "An advanced virtual flux integrated multifold table-based direct power control with delay compensation for active front-end rectifiers," *Int. Trans. Electr. Energy Syst.*, no. October, pp. 1–22, 2021, doi: 10.1002/2050-7038.13174.
- [6] A. Rath and G. Srungavarapu, "New Model Predictive Algorithm DPC based Shunt Active Power Filters (SAPFs)," *ICPEE 2021 - 2021 1st Int. Conf. Power Electron. Energy*, no. 3, pp. 48–53, 2021, doi: 10.1109/ICPEE50452.2021.9358550.
- [7] D. K. Choi and K. B. Lee, "Dynamic performance improvement of AC/DC converter using model predictive direct power control with

- finite control set," *IEEE Trans. Ind. Electron.*, vol. 62, no. 2, pp. 757–767, 2015, doi: 10.1109/TIE.2014.2352214.
- [8] P. Wang, Y. Bi, F. Gao, T. Song, and Y. Zhang, "An Improved Deadbeat Control Method for Single-Phase PWM Rectifiers in Charging System for EVs," *IEEE Trans. Veh. Technol.*, vol. 68, no. 10, pp. 9672–9681, 2019, doi: 10.1109/TVT.2019.2937653.
- [9] A. Rath and G. Srungavarapu, "Dead Beat Predictive DPC based Battery Charging System Using Dynamic DC-link Reference," pp. 01–06, 2022, doi: 10.1109/npec52100.2021.9672500.
- [10] T. Noguchi, H. Tomiki, S. Kondo, and I. Takahashi, "Direct power control of PWM converter without power-source voltage sensors," *IEEE Trans. Ind. Appl.*, vol. 34, no. 3, pp. 473–479, 1998, doi: 10.1109/28.673716.
- [11] J. Hu, J. Zhu, G. Lei, G. Platt, and D. G. Dorrell, "Multi-objective model-predictive control for high-power converters," *IEEE Trans. Energy Convers.*, vol. 28, no. 3, pp. 652–663, 2013, doi: 10.1109/TEC.2013.2270557.
- [12] S. Li and B. Ke, "Study of battery modeling using mathematical and circuit oriented approaches," *IEEE Power Energy Soc. Gen. Meet.*, pp. 1–8, 2011, doi: 10.1109/PES.2011.6039230.
- [13] W. Shen, T. T. Vo, and A. Kapoor, "Charging algorithms of lithium-ion batteries: An overview," *Proc. 2012 7th IEEE Conf. Ind. Electron. Appl. ICIEA 2012*, pp. 1567–1572, 2012, doi: 10.1109/ICIEA.2012.6360973.